Journal of the European Ceramic Society **18** (1998) 1663–1668

PII: S0955-2219(98)00086-7
0955-2219/98/$—see front matter

Relaxation of Indentation Residual Stress in Alumina: Experimental Observation by X-Ray Diffraction

Matteo Leoni,* Paolo Scardi and Vincenzo M. Sglavo

Dipartimento di Ingegneria dei Materiali, Università di Trento Via Mesiano 77, I-38050 Trento, Italy

(Received 2 October 1997; accepted 4 March 1998)

Abstract

The residual stress field generated by Vickers indentation in an alumina ceramic material was studied by an X-ray diffraction technique. A specifically designed stress/texture diffractometer was used to measure the residual strain at different locations around the indentation site, and the experimental values were compared with the theoretical stress field calculated on the basis of previous work. A compressive stress state was shown to prevail around the indentation site, the magnitude being a decreasing function of the distance from the contact point. The indented alumina specimens were then subjected to annealing treatments at temperatures up to 1000°C. The measurement of the stress field by the X-ray technique allowed the observation that the indentation residual stress can be completely removed by heat treatment at temperature around 900°C. © 1998 Elsevier Science Limited. All rights reserved

1 Introduction

Techniques based on the analysis of indentation cracks have been extensively used for the mechanical characterization of ceramic materials.[1] For example, fracture toughness can be easily calculated from the measurement of the length of the crack which develop from the corner of the indentation site, or from the strength evaluation of indented specimens.[2,3,4] In addition, the indentation test simulates particular events occurring in contact processes, thus furnishing useful information regarding the mechanisms which control fatigue, wear or strength loss. In order to analyse and quantify these phenomena, knowledge of the residual stress generated around the contact site is essential. The presence of a residual stress field around the indentation site usually complicates the interpretation of the results, especially when high temperature tests are performed. Some procedures have been proposed in order to calibrate experimentally the residual stress intensity factor associated to indentation cracks.[4,5,6,7] Nevertheless, the possibility of working with a stress-free controlled surface crack is appealing. In particular, it was proposed that indentation cracks could be 'unloaded' from the residual stress field: this can be performed either by the removal of surface layers of the material or by annealing treatments of the indented specimen.[4,7–11] In both cases, the definition of the conditions that allow a complete relief of residual stress is a formidable task. Measurement of the indentation residual stress field is a complicated issue, due to its localization around the contact site and to the contemporaneous presence of several stress components.

X-ray Residual Stress Analysis (XRSA) allows the non-destructive determination of residual stresses in polycrystalline materials.[12] This technique, which is commonly used for testing of metallic components, is not as popular for ceramics, essentially because of the small magnitude of the strains to be measured. This means that a particularly reliable instrumentation must be used to achieve high precision measurements.

The aim of the present work was to study the indentation residual stress field in alumina (90% pure) bars. The residual stress was measured by a specifically designed stress/texture diffractometer which allowed the stress trend around the indentation to be determined by measurements at different distance from the contact point. The indented alumina bars were then subjected to several heat

*To whom correspondence should be addressed.

treatments at temperatures up to 1000°C, in order to find the conditions of stress relaxation.

2 Experimental Procedure

Alumina bars (3 mm×4 mm×45 mm) from a commercial source (ALUBIT90, O. Bitossi, Italy) were used in this work. The chemical composition of the material was (wt%): 91·7 Al_2O_3, 6·2 SiO_2, 0·8 CaO, 0·5 MgO, 0·3 Na_2O, 0·5 other. The microstructure, shown in Fig. 1, mainly consisted of equiaxed grains with an average size around 5 μm; however, some elongated grains up to 20 μm can be observed. Grains were surrounded by an intergranular glassy phase which represents about 10% in volume. Residual porosity was below 0·1%. One of the 4 mm wide faces was polished with diamond paste up to 3 μm. Edges were chamfered following conventional procedure.

Vickers indentations were obtained in air using a maximum load equal to 294 N. Four indentations (4 mm apart) were made on the inner region of the bars which were eventually subjected to bending test. Only one indentation was produced on samples used for X-ray diffraction tests. Care was used in order to align the indentations with the specimen edges.

Some specimens were annealed at various temperatures up to 1000°C, in order to remove the residual stress field introduced by indentation. Heating and cooling rates as low as 2°C min^{-1} were used to this purpose.

X-ray diffraction (XRD) measurements were conducted on a Huber 4030 stress/texture diffractometer. The instrument is based on a parallel beam optic, realised through a graphite flat crystal monochromator and a 1 mm diameter collimator in the incident beam. The XRD patterns produced by the Cu Kα radiation, were collected by a position sensitive detector (PSD-Elphyse), which simultaneously detected a 2θ range of ~10°, with a step of 0·0102°. Typical counting time was 360 s for each pattern.

XRD patterns were collected on the indentation, and at increasing distance from it, by moving the beam as shown schematically in Fig. 2. The XRSA was performed by the $\sin^2\psi$ method,[12] which involves the collection of XRD patterns at different ψ-tilting. The geometry of the measuring system is also shown in Fig. 2.

Bending tests were performed by using a four-point bend fixture, with an inner and outer span equal to 20 and 40 mm, respectively. A constant cross head speed of 0·2 mm min^{-1} was used in these tests.

3 Results and Discussion

Figure 3 shows a high angle portion of the XRD pattern of an alumina bar collected by the PSD, with the indication of the Miller indices of the diffraction peaks. In order to determine the peak position with a high precision, which is a basic requirement for the XRSA, a numerical profile fitting program was employed. As shown in Fig. 3(b), the (31*10*) reflection was selected for the XRSA measurements, and the relevant X-ray Elastic Constants (XECs) were calculated from single crystal data, along the measured crystallographic direction, using the Hill average.[12]

The $\sin^2\psi$ method, used for the XRSA, is based on a simple model of biaxial stress field: this hypothesis is certainly approximate, but is reasonably appropriate in this case, considering the main purpose of our research, i.e. to find a simple analytical tool to study the stress relaxation conditions in indented samples. In addition, considering the shallow X-ray penetration, it must be noted that the biaxial stress hypothesis is frequently a good approximation. A further discussion on this point is reported in the following.

Figure 4 shows a typical ε versus $\sin^2\psi$ plot for a measurement on the indentation and 6·0 mm far from it, respectively. The positive slope of the trend for the measurement on the indentation clearly indicates the presence of an in-plane compressive

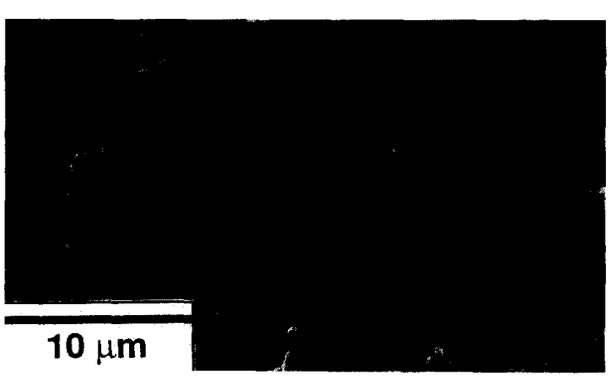

Fig. 1. Microstructure of the alumina studied in this work. A polished specimen was etched with HF solution to partially remove the grain boundary glassy phase.

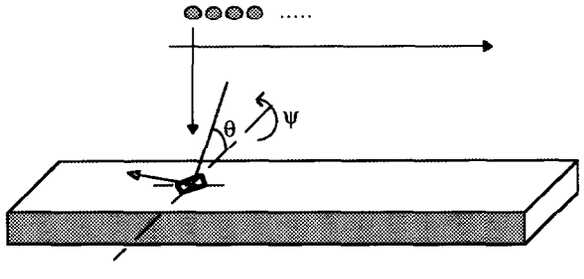

Fig. 2. Schematic of X-ray beam positioning with respect to the indentation site, with definition of ψ and ϕ angles.

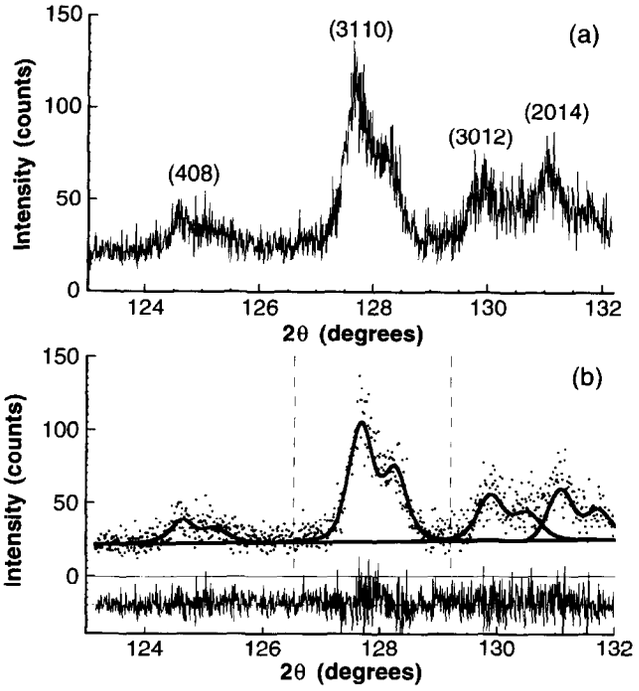

Fig. 3. XRD pattern collected by the PSD, with indication of Miller indices of the observed alumina peaks (a); profile fitting (b).

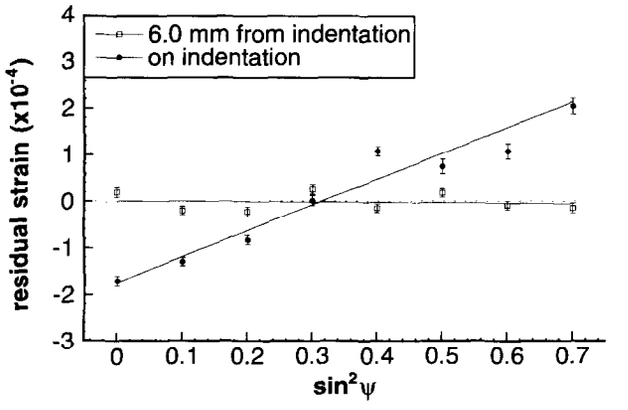

Fig. 4. Residual strain as a function of $\sin^2\psi$ ($\sin^2\psi$ plot) for two positions: indentation site (●) and 6·0 mm aside (□).

stress. No data 'splitting' for positive and negative ψ-tilting was observed within the experimental uncertainty, suggesting that the main stress component is in-plane. The residual stress was clearly zero far from the indentation, as confirmed by the zero slope for the 6·0 mm measurement. Therefore, it was possible to use the interplanar distance calculated from this measurement as the strain-free value of the (31*1*0) d-spacing, d_o. In this way the residual strain was entirely calculated from experimental data, at any ψ-tilting, as $\varepsilon = (d_y - d_o)/d_o$.

From these measurements and other ones at increasing distance from the indentation, it was possible to determine the residual stress profile shown in Fig. 5. This result is reported here to demonstrate the feasibility of such type of measurements; a better spatial resolution may be achieved by using collimators with a smaller diameter (0·3 mm or less), and by increasing the number of measurement points around the indentation accordingly.

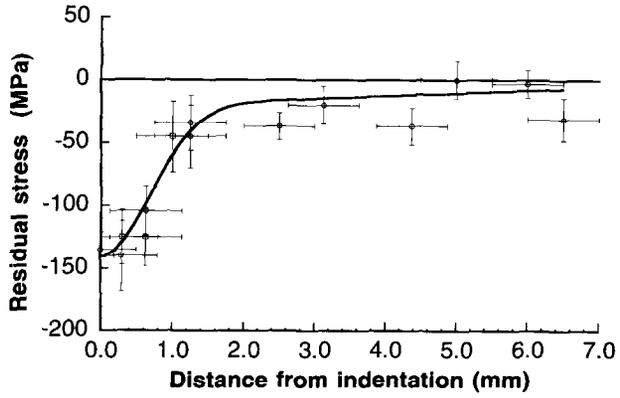

Fig. 5. Residual stress profile obtained from XRSA.

The stress profile in Fig. 5 can be compared with the theoretical stress field associated to a Vickers indentation. The stress components can be calculated on the basis of the results presented in previous works; Yoffe proposed that the stress acting outside the indentation after the load has been removed can be calculated as:[13,14]

$$\sigma(\rho, \phi) = \beta g(\phi)\frac{1}{\rho^3} \qquad (1)$$

where β represents the strength of the field, ρ and ϕ are defined in Fig. 6, and $g(\phi)$ is an angular function.[13] Sglavo and Green showed that β should be around 12–18 kPa mm^3 for a better agreement between theoretical and experimental stress field in soda-lime silicate glass.[14] This factor depends on the hardness of the material, H, and on the extension of the contact site, α, through the relation $\beta = \xi H a^3$, where ξ is a dimensionless constant.[13] On the basis of the results presented by Sglavo and Green, ξ can be evaluated around 0·20.[14] Therefore, as the hardness of the alumina bars was equal to 10·4 GPa,[4] a value of $\approx$1·78 MPa mm^3 can be used for the calculation of the residual stress field generated by indentation in the samples used in this work. On the basis of eqn (1) the principal stress components can be calculated. Figure 6 shows the contours of the principal stresses as a function of the distance from the indentation site in a general plane rotating around the indentation axis, y. It is important to point out that eqn (1) was determined for an axy-simmetric geometry.

In spite of the simple approximation involved by the $\sin^2\psi$ method, we can qualitatively compare the theoretical predictions with the XRSA results; a correct comparison, however, must consider that the XRSA is relevant to the outer layers only of the alumina bar. Moreover, due to the absorption of

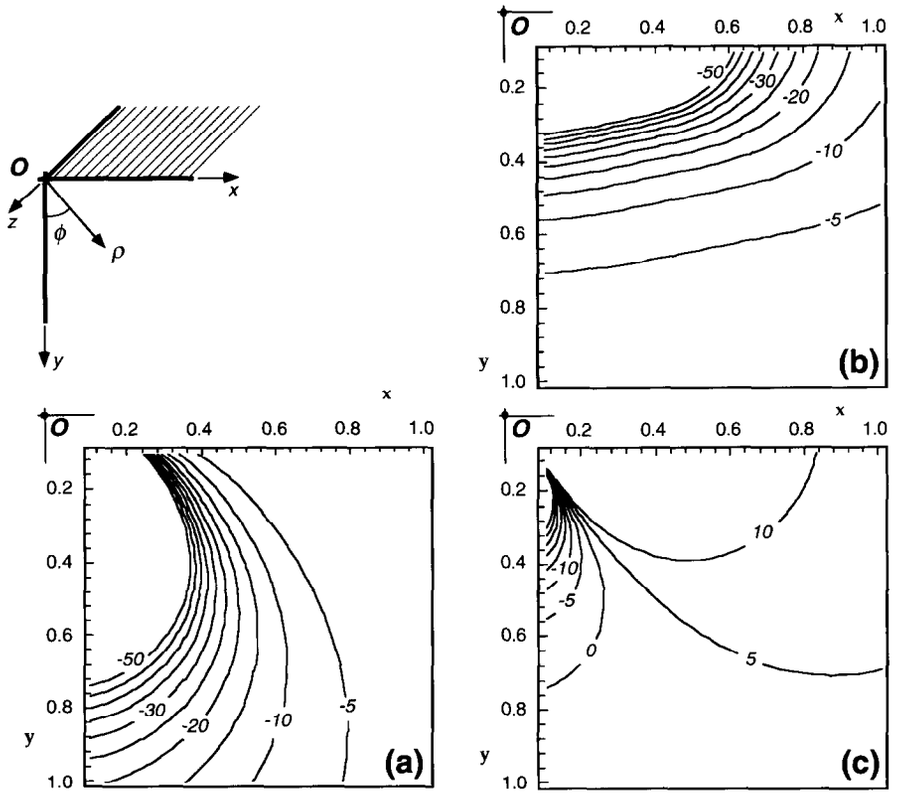

Fig. 6. Contours of the principal stresses around an indentation: (a) σ_{11}, (b) σ_{22}, (c) σ_{33}. Point O represents the initial contact point. Distances along the x, y axes are given in mm, stresses in MPa. The dashed plane (x,z) represents the indented surface.

the X-ray beam, the relative weight of layers at different depth decreases exponentially. The weight factor is

$$\exp\left(-\frac{2\mu \cdot y}{\sin\theta\cos\psi}\right) \qquad (2)$$

where y is the depth (see Fig. 6) and μ is the linear absorption coefficient. For our Al_2O_3 test bar $\mu = 120{\cdot}66\,cm^{-1}$, whereas $\theta \sim 64°$. As shown in Fig. 4, the ψ-tilting angle changes from 0 to 70° during the XRD measurements, therefore we can use a value of $\cos\psi = 0{\cdot}7(\psi = 45°)$ in eqn (2) to evaluate an average residual stress according to the theoretical model: the profile of the averaged stress components, S_{xx}, S_{yy}, S_{xy} and S_{zz}, is reported in Fig. 7. To have a reasonable numerical estimate of the thickness of material sampled by the X-ray beam, we can consider the equivalent thickness, $\tau_{eq} = (\sin\theta\cos\psi)/2\mu$, which is the thickness of a hypothetical non-absorbing layer giving the same amount of diffracted intensity as the actual absorbing (infinitely thick) material. Under the same conditions considered above, $\tau_{eq} \approx 26\ \mu m$.

Figures 6 and 7 show that a compressive stress state prevails around the indentation, the magnitude of the compressive stress decreasing with the distances from the contact site. In addition, S_{xx} substantially prevails on the other stress components. To this purpose, it is worth saying that XRSA refers to the corresponding strain component, ε_{xx}. Therefore, in spite of all the approximations, a good qualitative agreement can be observed between measured (Fig. 5) and calculated stress values (Fig. 7).

It is important to point out that the calculated stress can be compared with experimental results only outside the hardness impression. Due to the irreversible deformation (compaction and crushing) taking place beneath the indentation, strain can be considered as elastic only for distances from the contact site larger than $\approx 200\,\mu m$.[4] Besides approximations already introduced, discrepancies between the experimental and calculated trends can be imputed to several reasons. First of all, eqn (1) does not represent an exact analytical description of the stress field around an indentation, but terms with higher negative order in ρ should be taken into account for a higher precision in the calculations.[13] As already pointed out, the relations proposed by Yoffe[13] were derived for an axi-symmetric geometry, and therefore problems arising from the pyramidal shape of the indenter were neglected. In addition, as pointed out by Sglavo and Green, one single value of the parameter β does not allow to fit the measured indentation stress field.[14] Finally, the large spot size used for the XRSA could be another reason for the discrepancies between theoretical and measured stress values.

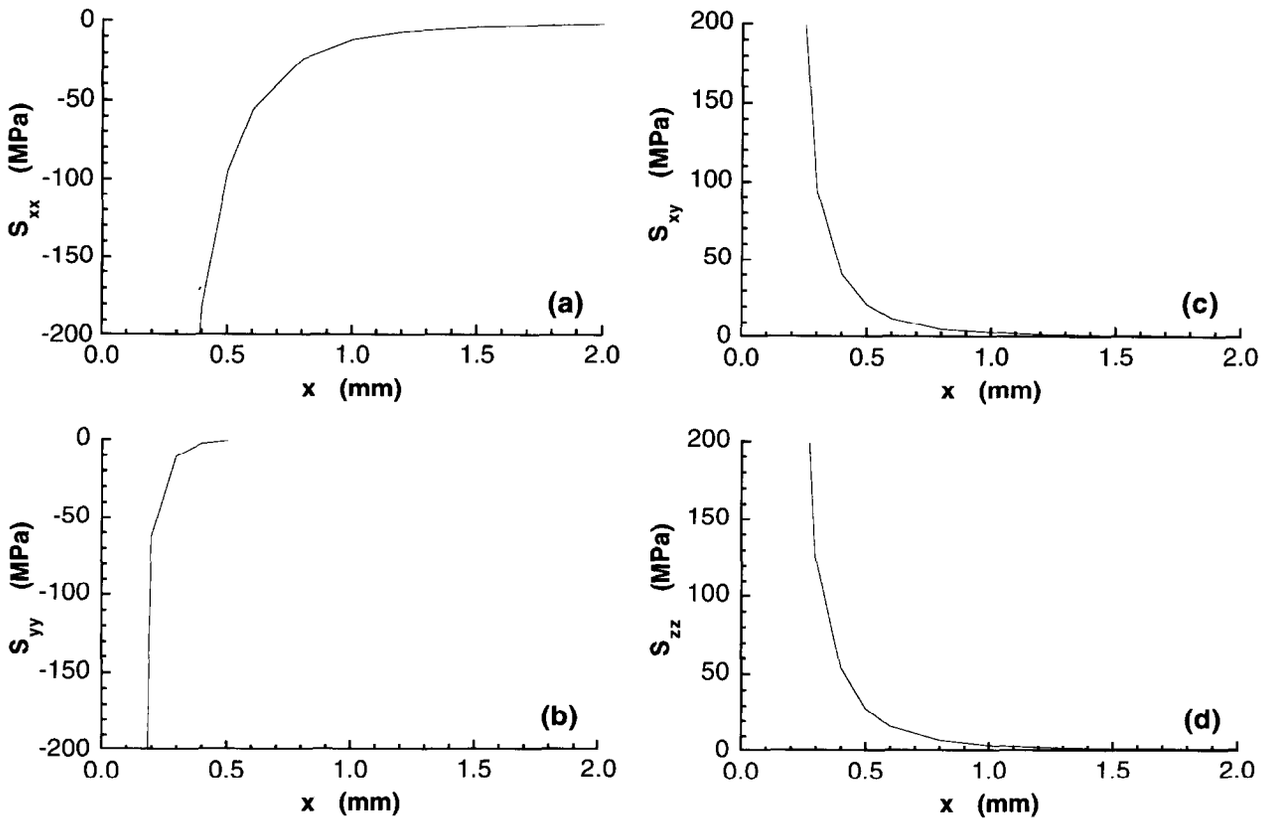

Fig. 7. Average stress components, calculated according to the exponential weight [eqn (2) in the text], as function of the distance from the contact site. (a) S_{xx}, (b) S_{yy}, (c) S_{xy} and (d) S_{zz}.

The relaxation of the residual stress was activated by heat treatment, taking advantage from the presence of a 10% of amorphous phase. In order to find the suitable conditions for stress relief, several thermal treatments were tested. All treatments were performed with a low heating and, specially, low cooling rates ($\approx 2°C\,min^{-1}$). As shown in Fig. 8, temperatures up to 800°C were ineffective: a complete stress relaxation was obtained only after a 2 h heat treatment at 900°C.

Therefore, in spite of the approximation in the stress analysis which adopted a simple biaxial stress model, the stress relief conditions could be determined as well as the stress profile near the indentation. Concerning the adequacy of the $\sin^2\psi$ method, the strain was observed to slightly deviate from the linearity in the $\sin^2\psi$ plot. This effect was increasingly visible for higher ψ-tilting and was easily detectable for $\sin^2\psi > 0{\cdot}7$. Above this value the slope decreased, thus indicating an overall curvature of the $\sin^2\psi$ diagram. This effect can be attributed to the presence of a stress gradient in the sampled volume,[12,15] with decreasing compression (and even a tension) towards the surface of the sample. The curvature could be used to calculate this gradient and the method is interesting when several measurements with different wavelength (i.e. different penetration depth) can be collected.[15] Further work, possibly employing synchrotron radiation, would be necessary to develop this methodology.

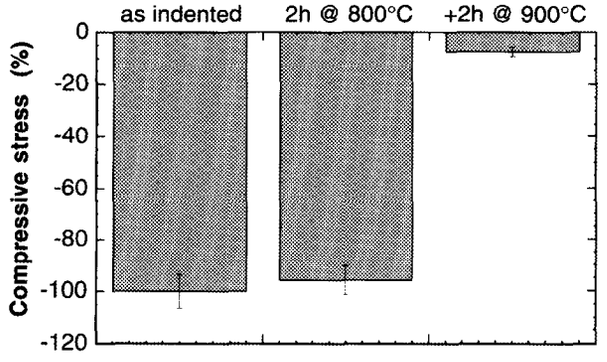

Fig. 8. Relief of residual stress on the indentation site after heat treatments: percentage reduction with respect to the as-indented alumina bar.

In order to understand the importance of a proper annealing procedure, bending strength of as-indented specimens was compared with the resistance of specimens annealed at 900°C. Results

Table 1. Strength, σ_f, initial surface crack length, c_0, and length at instability, c_m, in as-indented and annealed specimens

	as-indented	*Annealed*
σ_f (MPa)	83·2 ± 6·4	130·1 ± 4·1
c_0 (μm)	475 ± 16	448 ± 41
c_m (μm)	956 ± 80	465 ± 25

are reported in Table 1. The strength (σ_f) for as-indented bars is sensibly lower than for annealed samples. As a further and more specific proof of the residual stress removal by thermal treatment at 900°C, 'dummy' indentation cracks were analysed using a decorating technique described in a previous work.[4] As a matter of fact, the presence of the residual indentation stress field is responsible for a stable crack growth as the crack length doubles from c_0 to c_m (Table 1). Conversely, no evident stable crack growth could be detected in annealed specimens.[4] Therefore, stress-free defects can be produced in the alumina ceramic studied in this work by annealing at 900°C.

The data presented so far involve another important technological consequence regarding the presence of residual stress in ceramic materials. For example, it is well known that industrial grinding can be responsible for the formation of residual stresses on the surface of ceramic materials.[16] Such residual stresses can account for an increase in the strength and apparent fracture toughness of the material.[16] From this point of view, the XRSA technique presented in this work represents also a powerful tool for non-destructive measurement of machining-induced surface stresses in ceramic materials.

4 Conclusions

The residual stress field around Vickers indentations was measured on 10% glassy phase containing alumina by an X-ray stress analysis. The stresses were calculated on the basis of the residual strains of the (31*10*) Al_2O_3 peak shift. A compressive stress state was shown to prevail around the indentation, the magnitude of the stress being a decreasing function of the distance from the contact site. The analysis of the stress field on specimens annealed at different temperatures allowed to point out that the indentation stress field can be completely removed by a heat treatment at 900°C.

References

1. Lawn, B. R., *Fracture of Brittle Solids—2nd edn.* Cambridge University Press, Cambridge, 1993.
2. Anstis, G. R., Chantikul, P., Lawn, B. R. and Marshall, D. B., A critical evaluation of indentation techniques for measuring fracture toughness: I, Direct crack measurements. *J. Am. Ceram. Soc.*, 1981, **64**(9), 533–538.
3. Chantikul, P., Anstis, G. R., Lawn, B. R. and Marshall, D. B., A critical evaluation of indentation techniques for measuring fracture toughness: II, Strength method. *J. Am. Ceram. Soc.*, 1981, **64**(9), 539–543.
4. Sglavo, V. M. and Pancheri, P., Crack decorating technique for fracture toughness measurement in alumina, *J. Eur. Ceram. Soc.*, in press.
5. Dransmann, G. W., Steinbrech, R. W., Pajares, A., Guiberteau, F., Dominguez-Rodriguez, A. and Heuer, A. H., Indentation studies on Y_2O_3-stabilized ZrO_2: II, Toughness determination from stable growth of indentation-induced cracks. *J. Am. Ceram. Soc.*, 1994, **77**(5), 1194–1201.
6. Smith, S. M. and Scattergood, R. O., Crack shape effects for indentation fracture toughness measurements. *J. Am. Ceram. Soc.*, 1992, **75**(2), 305–315.
7. Bleise, D. and Steinbrech, R. W., Flat R-curve from stable propagation of indentation cracks in coarse-grained alumina. *J. Am. Ceram. Soc.*, 1994, **77**(2), 315–322.
8. Pajares, A., Guiberteau, F., Steinbrech, R. W. and Dominguez-Rodriguez, A., Residual stresses around Vickers indents. *Acta Met. Mater.*, 1995, **43**(10), 3649–3659.
9. Braun, L. M., Bennison, S. J. and Lawn, B. R., Objective evaluation of short-crack toughness curves using indentation flaws: Case study on alumina-based ceramics. *J. Am. Ceram. Soc.*, 1992, **75**(11), 3049–3057.
10. Marshall, D. B., Lawn, B. R. and Chantikul, P., Residual stress effects in sharp contact cracking. Part 2. Strength degradation. *J. Mater. Sci.*, 1979, **14**, 2225–2235.
11. Xu, H. H. K., Ostertag, C. P. and Krause Jr, R. F., Effect of temperature on toughness curves in alumina. *J. Am. Ceram. Soc.*, 1995, **78**(1), 260–262.
12. Noyan, I. C. and Cohen, J. B., *Residual Stress*. Springer Verlag, New York, 1987.
13. Yoffe, E. H., Elastic stress fields caused by indenting brittle materials. *Philos. Mag. A*, 1982, **46**, 617–628.
14. Sglavo, V. M. and Green, D. J., Subcritical growth of indentation median cracks in soda-lime-silica glass. *J. Am. Ceram. Soc.*, 1995, **78**(3), 650–656.
15. Scardi, P., Leoni, M. and Veneri, S., Residual stress analysis of ceramic coatings by means of synchrotron radiation XRD. *Adv. in X-ray Anal.*, in press.
16. Zhao, J., Stearns, L. C., Harmer, M. P., Chan, H. M., Miller, G. and Cook, R. F., Mechanical behaviour of alumina-silicon carbide 'nanocomposite'. *J. Am. Ceram. Soc.*, 1993, **76**(2), 503–510.
17. Chou, I. A., Chan, H. M. and Harmer, M. P., Machining-induced surface residual stress behavior in Al_2O_3-SiC nanocomposite. *J. Am. Ceram. Soc.*, 1996, **79**(9), 2403–2409.